Optimal Scheduling of a Large-scale Electrolyzer for Grid Services Provision and Renewable Sourced-Hydrogen Production

Sylvain Ledur, Robin Molinier, Simon Camal, Moulay-Driss Elalaouifaris, Georges Kariniotakis

Optimal Scheduling of a Large-scale Electrolyzer for Grid Services Provision and Renewable Sourced-Hydrogen Production

Sylvain LEDUR[a,b,*], Robin MOLINIER[b], Simon CAMAL[a], Moulay-Driss ELALAOUIFARIS[b], Georges KARINIOTAKIS[a]

[a]*Mines Paris, PSL University, Centre for processes, renewable energy and energy systems (PERSEE), 1 rue Claude Daunesse, Sophia Antipolis, 06904, France*

[b]*Air Liquide Research & Development, Paris Innovation Campus, 1 chemin de la Porte des Loges, Les Loges-en-Josas, 78350, France*

Abstract

Low-carbon hydrogen is expected to be crucial to the energy transition in the coming years. However, its production is not yet competitive with fossil-fuel-based hydrogen production. This paper proposes an economic analysis of an electrolyzer providing grid services combined with multi-market participation to fully exploit the flexibility potential of this technology. Optimization under uncertainty is combined with a rolling horizon algorithm to simulate the day-to-day trading decisions of the plant, first in a deterministic, then in a robust fashion. The impact of the multiple uncertainty sources on the production cost reduction is assessed. The case of German markets combined with the ENTSO-E harmonization project for secondary frequency reserve is considered. The effects of the 2021 energy crisis on the different strategies is also analyzed. The results show that both uncertain approaches behave similarly when adding the reserve, with a cash flow increase of around 10% before the crisis but a higher exposure to risk. The addition of reserve provision during the crisis drastically improves the performance of uncertain strategies with close to a 300% increase in cash flow. The robust approach greatly reduces the imbalances caused by wind power generation uncertainty compared to its deterministic counterpart. Finally, the addition of reserve provision induces a notable decrease in the green H2 breakeven price, but not enough to compensate for the costs associated with high electricity market prices.

Keywords: Ancillary Services, Robust Optimization, Low-carbon Hydrogen, Multi-market Electricity Provision, Industrial Flexibility

1. Introduction

With the increase in global warming and natural resources depletion, an energy transition has become inevitable for society. Increased renewable energy penetration in the energy mix is a major part of this energy transition. Variable Renewable Energy (VRE) sources introduce additional volatility into energy production. Power system flexibility has already been identified as one of the main levers to manage this supply volatility. In addition to reducing the amount of flexibility that can be provided by generators in the power system, VRE introduces increasing generation uncertainty and seasonal dependency into power generation Dudurych (2021).

Green hydrogen (H2) has been identified as critical for the ongoing energy transition IEA (2021b). However, as of today, means of H2 production are mostly carbonated and represent around 830Mt CO2/yr (2.5% of global CO2

*Corresponding author

Email addresses: sylvain.ledur@minesparis.psl.eu (Sylvain LEDUR), robin.molinier@airliquide.com (Robin MOLINIER), simon.camal@minesparis.psl.eu (Simon CAMAL), moulay-driss.elalaouifaris@airliquide.com (Moulay-Driss ELALAOUIFARIS), georges.kariniotakis@minesparis.psl.eu (Georges KARINIOTAKIS)

emissions) IEA (2019). Hydrogen currently has multiple uses, the main ones being oil refining and industry. However, to meet its "Net Zero Emissions by 2050" scenario, the IEA is expecting H2 demand to multiply almost sixfold by 2050 IEA (2021a). The goal is therefore not only to decarbonize existing means of H2 production, but to also increase the overall volumes produced. Among the solutions considered to decarbonize H2 production, two main techniques stand out, each with their own drawback. The first solution is water electrolysis powered by low-carbon electricity. The production costs of this type of green H2 are high, due to its dependency on electricity prices IRENA (2020). In addition, this solution needs to deal with supply volatility. The second solution is Carbon Capture and Storage (CCS), which retains the CO2 output at the cost of reducing the efficiency of the process Martínez-Rodríguez and Abánades (2020). In addition, SMR plants are themselves dependent on natural gas, which clashes with the objectives set by the European Commission regarding the reduction of dependency on natural gas imports Commission (2022).

In this paper, we put the focus on water electrolysis and the potential means of increasing its financial viability for green hydrogen production. In this context, two main technical challenges emerge.

First comes electricity supply volatility. The industrial consumer have to reduce its imbalances to the minimum, especially when considering grid services provision. Adding uncertainty in the form of a volatile energy supply brings difficulties in the management of the plant electricity profile.

The second challenge regarding water electrolysis is its production cost. The price of one kilogram of H2 produced from electrolysis is currently higher than one kilogram produced from fossil-fuel-based technologies (SMR for instance). While investment cost reduction can be expected as technology matures Seck et al. (2022), this requires time and heavy investments. In the meantime, cost reduction strategies have to be developed to facilitate the transition toward low-carbon H2 production.

The interest of building tools to exploit electrolysis flexibility with VRE supply is therefore twofold. First, it brings additional flexibility levers needed in the network to facilitate the increasing share of VRE in the electricity mix. Second, the revenues yielded by the provision of ancillary services from an electrolyzer powered with green electricity reduce the cost of producing green H2 and narrow the competitiveness gap with fossil-fuel-based H2.

H2 production is usually considered as a means to hedge the uncertainty resulting from VRE production Scolaro and Kittner (2022); Massana et al. (2022), rather than for the production of hydrogen itself. However, this results in small electrolysis plants not producing enough for large H2 consumers. Regarding larger plants producing H2 for industry, the question arises of the advantages of optimal flexible operation. In this paper, we simulate the day-to-day scheduling of electricity and the provision of grid-balancing services for a large-scale industrial electrolyzer powered by variable wind energy in order to assess the potential revenues of such a set-up and the impact of the various uncertain quantities on the achievable production cost of green H2.

1.1. Related Research

The ability of electrolyzers to provide Ancillary Services (AS) is extensively discussed in the literature. While the theoretical ramping of an electrolyzer could allow the provision of primary frequency reserve (or Frequency Containment Reserve, FCR), as investigated in Baetens et al. (2020); Dadkhah et al. (2021); Dozein et al. (2021); Samani et al. (2020), the impact of such a dynamic operation on cell degradation is not very well known. In Bergen et al. (2009) an electrolyzer is subject to large changes in power consumption for 30 seconds, with a 10 min frequency between events. This type of operation shows large amounts of degradation in the cell if the electrolyzer has no operating floor in terms of current, and normal degradation otherwise. Similar conclusions are drawn in Weiß et al. (2019). Based on the assumption that the activation of a secondary frequency reserve (automatic or manual Frequency Restoration Reserve, respectively aFRR and mFRR) will not require ramp changes within less than 30 sec when activating an asset, there is no need for a degradation model accounting for the dynamic operation of the electrolyzer.

In Dadkhah et al. (2022), the comparison of potential revenues coming from the three types of frequency reserve (FCR, aFRR, and mFRR) is considered in the context of investment in a hydrogen refueling station. Under the authors' assumptions regarding uncertainty and market modeling, it appears that automatic secondary reserve (aFRR) is the most profitable of the three options. These assumptions do not however consider the sequential uncertainties resulting from the interactions between the various markets and services. These sequential uncertainties can be handled in several ways.

Nomenclature

Variables:		**Indices:**	
Q	Flow (Nm3)	$(\cdot)^{DA}$	Day-ahead
P	Power (MW)	$(\cdot)^{ID}$	Intra-day
E	Energy (MWh)	$(\cdot)^{PPA}$	Power Purchase Agreement
C	Cost (€)	$(\cdot)^{Re}$	aFRR Reserve
R	Revenue (€)	$(\cdot)^{ELY}$	Electrolyzer
λ	Price (€/MW)	$(\cdot)^{cbid}$	Capacity Bid Price (€/MWh)
Parameters:		$(\cdot)^{ce}$	Clearing Energy Price
V	Sell Value (€/kg)	$(\cdot)^{\uparrow\downarrow}$	Participation Direction
h	Period length	$(\cdot)^{C}$	Contracted Reserve
K_{eff}^{H2}	ELY Efficiency (MWh/kgH2)	$(\cdot)^{NC}$	Non-Contracted Reserve

In Wu et al. (2021), an H2 refueling station uses multi-stage stochastic programming to handle the sequential uncertainty resulting from multi-market and reserve participation. The authors do not however consider the possibility of not being scheduled for reserve. In Al-Lawati et al. (2021), a set of two-stage stochastic optimization problems is used to operate a VRE plant in a sequential energy market context. Running the multiple problems together allows the re-actualization of the data used for decision-making within the process but induces a heavier computational burden.

Rolling horizon approaches can also be used to manage sequential uncertainties. In the context of scheduling the operation of a plant, a rolling horizon approach allows simpler models to be run consecutively over time in order to decrease the computational costs Sahin et al. (2013). The same simpler optimization problem can be run consecutively simply by changing the input, therefore actualizing the uncertain quantities as the lead times change Ziarnetzky et al. (2018). Applied to sequential electricity markets, this approach allows for the modeling of known and unknown information regarding the gate closure and positions on the various markets and mechanisms. It also accounts for the changing lead times in the forecasts that affect decision-making when it comes to VRE Ding et al. (2015). Thanks to the use of rolling horizon methods, the varying forecast lead-times can be handled and the uncertain parameters can be managed through the repeating optimization problem.

Optimization under uncertainty is a well-researched field. Stochastic optimization can be used to manage the uncertain inputs, either through synthetic scenarios Dadkhah et al. (2022), or using past data Wu et al. (2021). This method however involves a large computational burden and requires scenario reduction techniques. In addition, it computes an average revenue over a period. When considering plants with operational constraints, one also needs to make sure that the operation of the plant will be feasible regardless of the realization of the uncertain parameters. To do so, robust optimization can be used. In Wang et al. (2017), robust optimization is applied to manage the uncertainty of wind and solar power in the context of a microgrid with joint energy and reserve participation. In Gu et al. (2019), a robust formulation handles wind power uncertainty in the context of power-to-gas hydrogen injection into natural gas pipelines. Robust optimization tends to represent less of a computational burden due to the absence of scenarios,

which makes it more appropriate in the context of a rolling horizon algorithm with multiple iterations of similar optimization problems.

To summarize, sequential uncertainties can be modeled inside the optimization model itself through multistage stochastic optimization, or outside by running the optimization model within a rolling horizon algorithm. The latter has the advantage of being less computationally heavy and more tractable. In addition, the rolling horizon allows an easy switch between deterministic robust optimization problems, which presents an advantage when comparing both methods. The rolling horizon combined with an optimization problem approach will therefore be used in this work.

1.2. Key contributions

The main goal of this work is to simulate the day-to-day trading of a large-scale industrial Proton Exchange Membrane (PEM) electrolyzer providing secondary reserve to reduce the production cost of green hydrogen. Using close to real-life market modeling assumptions, we assess the impact of market quantities and wind power sourcing uncertainties on the overall revenue generation. The rules of the ENTSO-E aFRR framework PICASSO ENTSO-E (b) are used to model the secondary reserve provision, including the possibility to participate with non-contracted energy bids. This framework is presented in Section 3.2. The main contributions of this paper are:

- By considering a large-scale electrolyzer (hundreds of MW) producing H2 for industrial use rather than the usual smaller-scale plants considered for either refueling stations or to hedge wind power plant uncertainty, we assess how profitable secondary reserve provision could be when operating a plant large enough not to be limited by rules of participation in the market and services.
- A robust optimization problem is embedded in a rolling horizon algorithm to handle the evolution of information throughout the day and hedge the risk associated with forecasting errors. The trading behavior and decision-making of the plant are represented in a close to real-life way. Each market and service is modeled following the related gate closure and bid rules, and the PPA modeling is set to correspond to a potential PPA contracting for industrial application.
- The competitiveness of green hydrogen is analyzed based on various production and trading strategies. Applying evolving uncertainty management, we assess the impact of unknown quantities, which allows us to formulate green H2 break-even price ranges that can be compared to the price of gray hydrogen.
- Risk management analyses are performed to assess the exposure to extreme events for each trading strategy and optimization approach.

This paper is organized as follows. Section 2 presents the methodology of the work. In Section 3, the modeling assumptions and rules associated with the multi-market participation and balancing services provision are introduced. The deterministic and robust formulations of the optimization problem are then presented in Section 4. Section 5 describes the use-case considered in this work. Finally, Section 6 presents the results of the simulation and their analysis.

2. Methodology

This section presents the methodology used to model the day-to-day operation of this electrolyzer. First, the model of the electrolyzer itself is described, followed by the characteristics of the PPA contract and the electricity markets and services. Finally, the optimization and rolling horizon approaches are presented.

2.1. Electrolyzer model and H2 production

When modeling the behavior of an electrolyzer, it is important to consider the non-linearities of this process. In the literature, the relationship between the electricity input and the hydrogen output for this type of plant is very often simplified to a constant value regardless of operating modes. In Baumhof et al. (2023), the authors challenge this simplistic modeling approach. It is shown that adding segments of piece-wise linearization does indeed increase the final revenue. However, it also adds new binary variables and increases the computational burden. Here we keep the

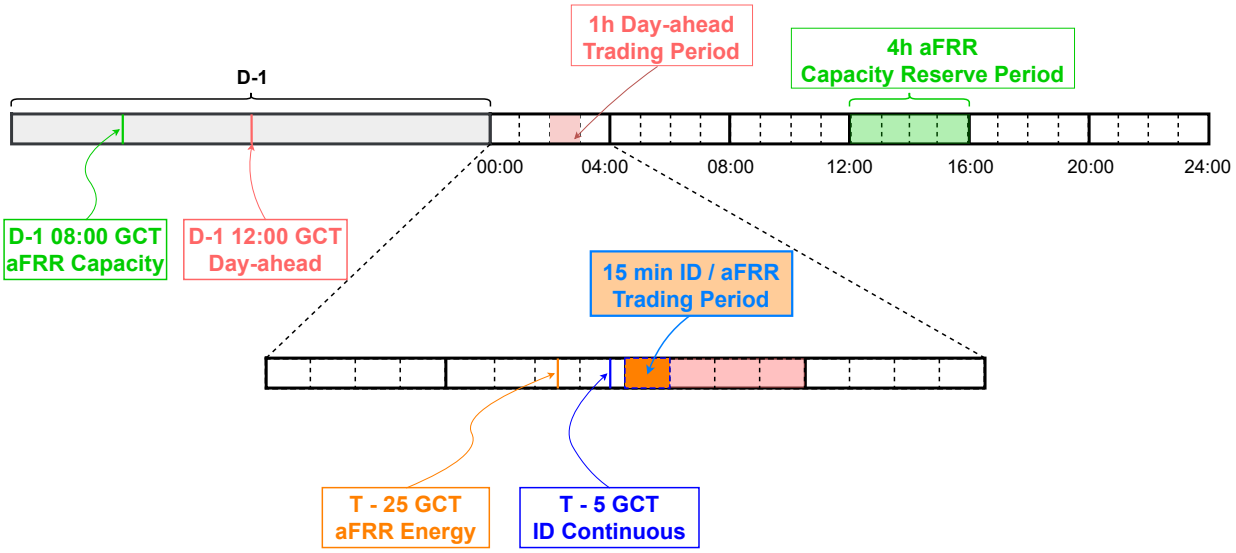

Figure 1: Trading timeline

constant ratio assumption to ensure tractability of the problem, but it is worth noting that increasing the complexity of the electrolyzer modeling while ensuring tractability of the simulation would add a worthwhile perspective to this work.

Regarding the power ramping of the electrolyzer, the PEM water electrolysis technology is highly flexible and we assume that the available ramp is similar to the rated power. In other words, we can change the set point of the asset from 0 to 100% of the rated power almost instantaneously.

$$P_t = \frac{1}{h} Q_t^{H2} K_{eff}^{H2} \tag{1}$$

The power coming from renewable sources produces green H2, while any other source of electricity (grid or reserve) will count toward gray H2 production.

2.2. Wind power PPA contract

As the main electricity source, direct access is granted to a wind farm producer in the form of a Power Purchase Agreement (PPA) contract. PPAs can take many forms depending on various contractual aspects. The wind power production is forecasted using numerical weather predictions combined with a random forest approach. The assumptions regarding the contractual aspects of the PPA production and the production forecast are investigated in Section 5.

2.3. Electricity markets and balancing mechanisms

A multi-market approach is taken when looking at electricity sourcing other than the PPA. The plant participates on the day-ahead market and in intraday continuous auctions to benefit from low prices when producing gray H2. It also provides secondary frequency reserve. This reserve mechanism is modeled following the German rules for the capacity auctions and the rules of the ENTSO-E PICASSO project for the energy auctions. The trading timeline with the various gate closures is represented in Figure 1. The rules and modeling assumptions regarding markets and balancing mechanisms are presented in detail in Section 3.

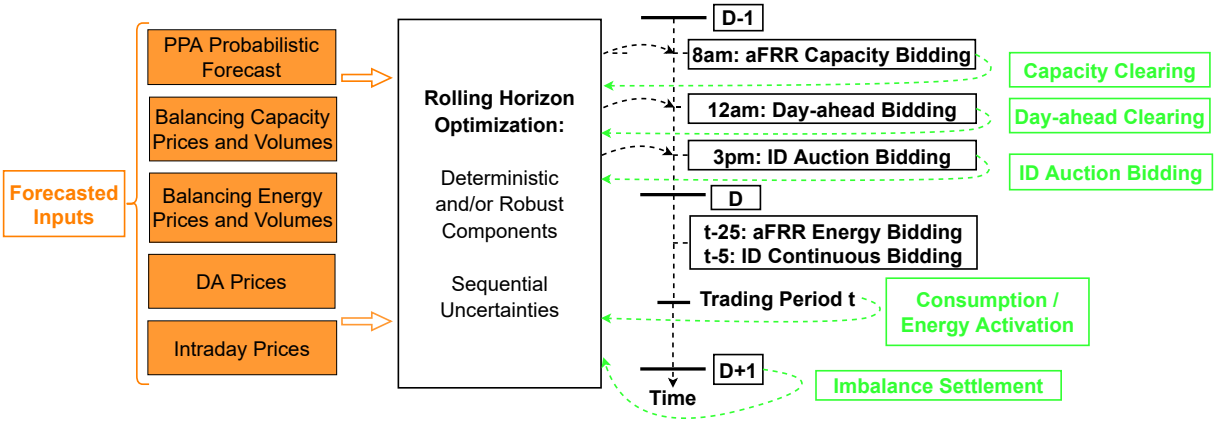

Figure 2: Optimization problem organization

2.4. Optimization and rolling horizon approach

The day-to-day scheduling of the plant is modeled using an optimization problem. This optimization returns optimal positions on the various markets, based on the imperfect knowledge used as input. The formulation is presented in Section 4. One should keep in mind that uncertainties vary depending on the lead time and the time of day considered. To account for this and the impact of the different market gate closure times, we develop a rolling horizon algorithm. Its goal is two-fold. First, it provides a model with realistic knowledge patterns. By running the rolling horizon over multiple periods, we simulate the chain of decisions the plant operator would have to take during the day. The algorithm can therefore adapt market bids and operational set points in line with the knowledge unlocked by passing a certain gate closure (as shown on the right side of Figure 2). Second, it simplifies the modeling for the analysis because the horizon of the optimization will be shorter and the separation between what is known and what is uncertain can be done beforehand while running the algorithm. A flowchart of the algorithm is shown in Figure 3. The chain of decisions changes based on which timestep is considered first in the algorithm to account for market positions after gate closure. Similarly, the forecasts are set accordingly, depending on which time of day the algorithm is considering (not shown in the algorithm flowchart for the sake of readability). In addition to the first trading period, an additional period representing the last known realization is added to compute the effective energy activation for the aFRR mechanism.

3. Electricity Markets and ENTSO-E Balancing Framework for aFRR

With the various changes coming to electricity trading and networks all over Europe, mostly due to an increasing share of VRE, electricity markets and ancillary services are evolving. This evolution brings new opportunities for industrial flexibility, with a general lowering of product resolution, and an opening of markets to demand-side participants.

In the past, European countries had their own way of providing balancing services for their own network. Most countries keep the same general structure (primary, secondary, and tertiary reserves), with different clearing mechanisms, standard products, settlement period length, and only certain types of actors admitted in the market as participants. In recent years, the ENTSOE (European Network of Transmission System Operators for Electricity) has developed a set of guidelines for a pan-European electric network that would ensure stability of the interconnected power system, in all time frames. Some, like the primary reserve, are already running at a European scale, while the others are expected to come online in the coming years. This paper focuses on Automatic Frequency Restoration Reserves (aFRR). In addition to system services, electricity markets are also considered in this work.

3.1. Day-ahead and intraday markets: rules and modeling assumptions

DA market participation is mainly characterized by the gate closure time (D-1 12:00), the bid energy, and time granularity (1-hour periods with a 1 MWh bid resolution). After the gate closure, the positions chosen by the plant are fixed

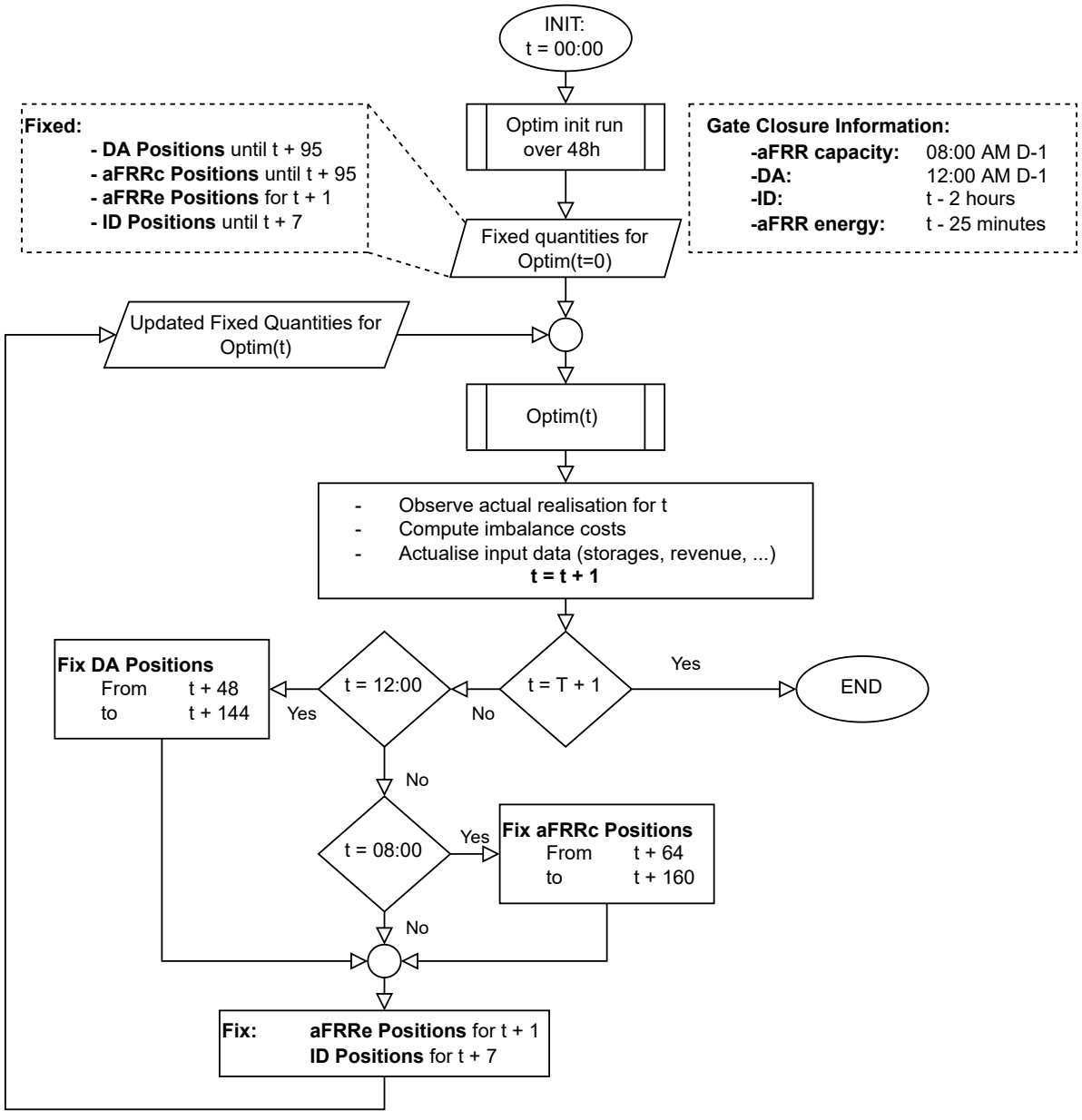

Figure 3: Rolling horizon algorithm flowchart showing the blocking of the positions on the various markets and mechanisms

and have to be respected. The intraday market constraints are similar but more flexible, with a bid energy granularity of 0.1 MWh, a period length of 15 min, and a gate closure time set at T-5 min. In addition to the rules relative to the participation on the markets, grid usage also has to be considered (see Section 5 for the specific use-case).

3.2. ENTSO-E aFRR framework: rules and bidding

In this section, the ENTSO-E aFRR framework is introduced. A particular feature of this aFRR framework is the combination of contracted (C) and non-contracted (NC) participation. This is a major aspect of the new framework, as it allows the Balancing Service Provider (BSP) to participate with balancing energy without a prior capacity reserve. It also means that the capacity price and energy price are decoupled and have two different gate closure times. First, the capacity reserve mechanism is presented for contracted participation. Next, the energy reserve bids and the energy activation mechanism are presented. Figure 4 shows an overview of the aFRR mechanism for both contracted and non-contracted participation.

Contracted capacity bidding: The ENTSO-E aFRR mechanism only considers energy activation. Therefore, the capacity reserve mechanism is still dependent on the country considered. German rules are considered in this work. The Gate Closure Time (GCT) for capacity bids is set at D-1 08:00. The bids take the shape of the following tuple: (Reserve Power (MW), Capacity Price (€/MW)). The bid validity period is 4 h. Capacity reserve acceptation follows a merit order clearing process driven by the capacity price. When a capacity reserve bid is accepted, the BSP must send contracted energy bids for each 15-min period within the 4h reserve period. The remuneration for capacity reserve is set in a pay-as-bid fashion.

Energy bidding: Regarding energy bids, both contracted and non-contracted bids follow the same rules. The gate closure time is set at T-25 min. Energy bids take the shape of the following tuple: (Reserve Power (MW), Energy Price (€/MWh)). The bid validity period is 15 min. For contracted bids, the reserve power in this tuple must be the same as the reserve power of the accepted capacity bid if the contracted bid were accepted. Non-contracted energy bids can be sent or not for any given period, as long as the gate closure constraint is respected.

Energy bid activation: The ENTSO-E framework runs a real time optimization for aFRR energy activation. As of now, the optimization cycle is set at 4 sec. An activation signal is sent to the BSP every 4 sec to indicate whether they have to activate their asset or not to balance the system. The energy bids are gradually activated based on the real-time imbalance needs of the system. This gradual activation follows the merit order curve formed by the prices of the energy bids (both contracted and non-contracted). Depending on its position in the merit order list, each bid has a certain imbalance threshold past which it is activated (if a bid is placed at 600 MW in terms of cumulative volumes on the merit order line, then it is activated if the imbalance reaches 600 MW or more). Every 4 sec a certain number of bids are activated based on the target signal. The full activation time is 5 min (supposed to be enforced by December 2024 ENTSO-E (2021)), which means that for a given order, the BSP has a maximum of 5 min to reach the total capacity offered. Energy bid remuneration is based on a pay-as-clear fashion. A different clearing is done every 4 seconds based on which bids are activated due to the real-time imbalance. Therefore, the marginal price for a given 15-minute period is the volume weighted average of the marginal prices for each 4-second period in which a given BSP is activated.

3.3. ENTSO-E aFRR framework: modeling assumptions

When modeling aFRR participation and bid activation, a few assumptions have to be made and fixed policies have to be set.

The two assumptions presented in this section are related to the energy activation mechanism. They are as follows:

- The activation signal data is not available, as the framework itself has not been put into place yet. A simulated signal has to be used.
- An assumption has to be made regarding whether a BSP can be only partially activated for its energy bids, or if the activation signal automatically activates all of the available reserve.

Activation signal: In order to simulate the activation signal, the second based aFRR target signal published by the German TSOs is used. This signal is averaged every 4 sec, resulting in a 4-second-based signal. This second based

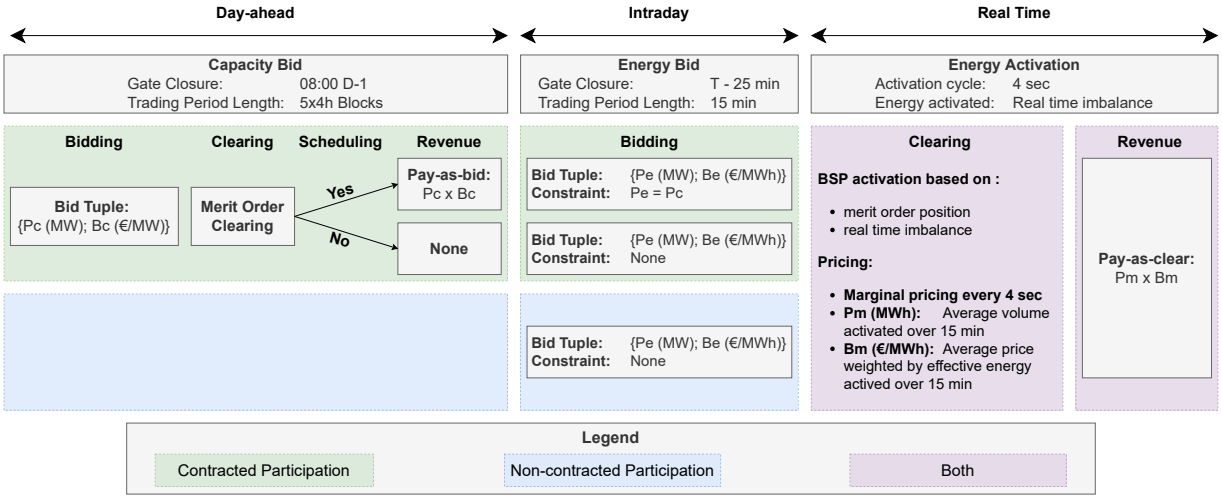

Figure 4: aFRR bidding and activation process

signal represents the real-time imbalance of the German grid, and is therefore the closest to the actual aFRR signal sent by the TSO. This signal is available on the German balancing website Regelleistung.

Partial activation: In this work, the assumption is made that if a bid is activated for energy balancing, it is fully activated.

4. Optimization Model

This section presents the deterministic optimization model used to produce the optimal scheduling of the electrolyzer.

4.1. Objective function

In the objective function, the costs of electricity transactions are minimized, while the revenues from hydrogen and secondary reserve provision are maximized.

$$\underset{\Omega}{\text{minimize}} \sum_{t} C_t^{ELEC} - R_t^{aFRR\uparrow\downarrow} - R_t^{H2} \tag{2}$$

$$\Omega = \{P_t^{DA},\ E_t^{aFRR},\ P_t^{ID}, Q_t^{H2} \in \mathbb{R}, \quad P_t^{Re\uparrow\downarrow} \in \mathbb{N}\}$$

4.2. Electricity markets transactions

The electricity transactions include the day-ahead and intraday markets participation, the amount of electricity received from the PPA, and the imbalance costs. It should be noted that the imbalance costs are both considered positive to penalize the objective function should they occur. The imbalance price λ^{IMB} cannot be known when running the optimization and is therefore set to an arbitrary amount high enough to only consider putting the system out of balance as a last resort. The actual imbalance costs are computed in post-processing when extracting the results of the optimization.

$$\begin{aligned} C_t^{ELEC} = h(&\lambda_t^{DA} P_t^{DA} + \lambda_t^{PPA} \tilde{P}_t^{PPA} \\ &+ \lambda_t^{ID}(P_t^{ID,Buy} - P_t^{ID,Sell})) \\ &+ \lambda^{IMB} P_t^{IMB\uparrow\downarrow} \end{aligned} \tag{3}$$

4.3. Electrolyzer operational constraints

The power consumed by the electrolyzer is represented by Equation (5). Equations (7) and (8) represent the power boundaries of the electrolyzer. In these two equations, the power imbalance is added to allow the system to go out of balance. This imbalance power is penalized in the objective function, as previously mentioned. Equations (9) and (10) represent the relationship between both green and gray H2 outputs. Downward reserve electricity cannot be counted as green supply, it will therefore count toward gray H2 production. A symbolic split between green and gray electricity is however made to represent the fact that the power sent to the grid for upward regulation can impact either green or gray H2 output. This split does not represent any physical differentiation of flux and is only used for modeling purposes (green certification is based on guarantees of origins accompanying the PPA volumes). The energy activation formulation is presented in the next section. The ELY ramping constraints are presented in equations (11) and (12).

$$P_t^M = P_t^{DA} + P_t^{ID,\,Buy} - P_t^{ID,\,Sell} \tag{4}$$

$$P_t^{Re\downarrow} = P_t^{Re\downarrow,\,C} + P_t^{Re\downarrow,\,NC} \tag{5}$$

$$P_t^{Re\uparrow} = P_t^{Re\uparrow,\,C} + P_t^{Re\uparrow,\,NC} \tag{6}$$

$$P_t^M + \tilde{P}_t^{PPA} + P_t^{Re\downarrow} - P_t^{IMB\downarrow} \leq P_{MAX}^{ELY} \tag{7}$$

$$P_t^M + \tilde{P}_t^{PPA} - P_t^{Re\uparrow} + P_t^{IMB\uparrow} \geq P_{MIN}^{ELY} \tag{8}$$

$$\begin{aligned} Q_t^{H2,\,gray} K_{eff}^{H2} = h(&P_t^{DA} + P_t^{ID,\,Buy}) \\ &+ E_t^{Re\downarrow} - E_t^{Re\uparrow,\,gray} \end{aligned} \tag{9}$$

$$\begin{aligned} Q_t^{H2,\,Green} K_{eff}^{H2} = h(&\tilde{P}_t^{PPA} - P_t^{ID,\,Sell}) \\ &- E_t^{Re\uparrow,\,Green} \end{aligned} \tag{10}$$

$$\begin{aligned} P_{Ramp\uparrow}^{ELY} \geq (&P_{t+1}^M + \tilde{P}_{t+1}^{PPA} + P_{t+1}^{Re\downarrow}) \\ &- (P_t^M + \tilde{P}_t^{PPA} - P_t^{Re\uparrow}) \end{aligned} \tag{11}$$

$$\begin{aligned} P_{Ramp\downarrow}^{ELY} \geq (&P_t^M + \tilde{P}_t^{PPA} + P_t^{Re\downarrow}) \\ &- (P_{t+1}^M + \tilde{P}_{t+1}^{PPA} - P_{t+1}^{Re\uparrow}) \end{aligned} \tag{12}$$

4.4. aFRR energy activation and revenues

The energy activation constraints are presented in equations (13), (15) and (16). The ratio β represents the activation ratio for a given period t which, once multiplied by the reserve power and the factor h, gives the exact energy activation for period t. The aFRR revenue is represented by Equation (17). And finally, Equation (18) represents the revenue earned from the production of both green and gray H2.

$$E_t^{Re\downarrow} = h(\beta_t^{\downarrow, C} P_t^{Re\downarrow, C} + \beta_t^{\downarrow, NC} P_t^{Re\downarrow, NC}) \tag{13}$$

$$E_t^{Re\uparrow} = E_t^{Re\uparrow, Green} + E_t^{Re\uparrow, gray} \tag{14}$$

$$E_t^{Re\uparrow, Green} = h(\beta_t^{\uparrow, C} P_t^{Re\uparrow, Green, C} + \beta_t^{\uparrow, NC} P_t^{Re\uparrow, Green, NC}) \tag{15}$$

$$E_t^{Re\uparrow, gray} = h(\beta_t^{\uparrow, C} P_t^{Re\uparrow, gray, C} + \beta_t^{\uparrow, NC} P_t^{Re\uparrow, gray, NC}) \tag{16}$$

$$R_t^{aFRR} = \lambda_t^{cbid\uparrow} P_t^{Re\uparrow, C} + \lambda_t^{ce\uparrow} E^{Re\uparrow} + \lambda_t^{cbid\downarrow} P_t^{Re\downarrow, C} - \lambda_t^{ce\downarrow} E^{Re\downarrow} \tag{17}$$

$$R_t^{H2} = V_t^{H2,Green} Q_t^{H2, Green} + V_t^{H2, gray} Q_t^{H2, gray} \tag{18}$$

4.5. Market rules

When considering 15-minute periods, both the day-ahead and capacity reserve markets have to be considered due to their larger trading time blocks. Equation (19) ensures that for all t within a given hour, all the power consumptions have to be the same. Similarly, Equation (20) ensures that all the offered power reserves are the same for each 4-hour trading block.

$$P_t^{DA} = P_{t-t\%\frac{1}{h}}^{DA} \qquad \forall\, t \,|\, t\,\%\,\frac{1}{h} \neq 0 \tag{19}$$

$$P_t^{Re\uparrow\downarrow, C} = P_{t-t\%\frac{4}{h}}^{Re\uparrow\downarrow, C} \qquad \forall\, t \,|\, t\,\%\,\frac{4}{h} \neq 0 \tag{20}$$

4.6. aFRR / ID direction

Finally, the ELY can only participate in one direction at a time in both the secondary reserve and intraday markets. This is represented by equations (21) to (24) using binary variables δ.

$$P_t^{Re\uparrow} \leq \delta^{Re, dir} M \tag{21}$$

$$P_t^{Re\downarrow} \leq (1 - \delta^{Re, dir}) M \tag{22}$$

$$P_t^{ID, Sell} \leq \delta^{ID, dir} M \tag{23}$$

$$P_t^{ID, Buy} \leq (1 - \delta^{ID, dir}) M \tag{24}$$

4.7. Locked market positions

To model the settled positions on a given market past its gate closure time, additional constraints are introduced to ensure the correct power levels for the corresponding time window. The information regarding which position is locked for which market and the position itself are stored in the matrices Θ^{GCT} and $\Theta^{Positions}$ respectively, both of dimension TxN with T the number of timesteps and N the number of markets considered.

$$\Theta_{t,n}^{GCT} = \begin{cases} 1 & \text{if } t \geq \text{GCT for market } n \\ 0 & \text{Otherwise} \end{cases} \tag{25}$$

Using this information, the fixed positions for each market are forced to match the scheduled amount through the constraints shown in (26).

$$P_t^n = \Theta_{t,n}^{Positions}, \quad \forall n,\ \Theta_{t,n}^{GCT} > 0 \tag{26}$$

4.8. Robust reformulation

A robust reformulation of the optimization problem is done to account for the uncertain generation of the PPA Gorissen et al. (2015). The uncertain generation is associated with a box uncertainty (obtained from probabilistic forecasts) as follows:

$$\tilde{P}_t^{PPA} \in [\underline{P_t}^{PPA},\ \overline{P_t}^{PPA}]$$

The reformulation can be simplified to remove the dual variables and additional constraints, leaving only eqs. (27) to (32) (Only the constraints containing the uncertain parameter P_t^{PPA} and P_{t+1}^{PPA}):

$$\begin{aligned} C_t^{ELEC} \geq\ & h(\lambda_t^{DA} P_t^{DA} + \lambda_t^{PPA} \overline{P_t}^{PPA} \\ & + \lambda_t^{ID}(P_t^{ID,Buy} - P_t^{ID,Sell})) \\ & + \lambda^{IMB} P_t^{IMB\uparrow\downarrow} \end{aligned} \tag{27}$$

$$Q_t^{H2,Green} K_{eff}^{H2} \leq h(\underline{P_t}^{PPA} - P_t^{ID,Sell}) \tag{28}$$

$$P_t^M + \overline{P_t}^{PPA} + P_t^{Re\downarrow} - P_t^{IMB\downarrow} \leq P_{MAX}^{ELY} \tag{29}$$

$$P_t^M + \underline{P_t}^{PPA} - P_t^{Re\uparrow} + P_t^{IMB\uparrow} \geq P_{MIN}^{ELY} \tag{30}$$

$$\begin{aligned} P_{Ramp\uparrow}^{ELY} \geq\ & (P_{t+1}^M + \overline{P_{t+1}}^{PPA} + P_{t+1}^{Re\downarrow}) \\ & - (P_t^M + \underline{P_t}^{PPA} - P_t^{Re\uparrow}) \end{aligned} \tag{31}$$

$$\begin{aligned} P_{Ramp\downarrow}^{ELY} \geq\ & (P_t^M + \overline{P_t}^{PPA} + P_t^{Re\downarrow}) \\ & - (P_{t+1}^M + \underline{P_{t+1}}^{PPA} - P_{t+1}^{Re\uparrow}) \end{aligned} \tag{32}$$

5. Use-case Presentation

In this work, a large-scale Proton Exchange Membrane (PEM) electrolyzer integrated into an industrial H2 network is considered noa. Certified green hydrogen produced by the plant can be sold as such in the industrial processes connected to the H2 network. This network is mainly fed through gray hydrogen production units such as SMR plants. It is assumed that the flow of H2 in the network is constant, large enough, and has sufficient other H2 production technologies for the output flow of the electrolyzer to be injected seamlessly without a need for storage. This electrolyzer is connected to a wind power plant through a PPA contract. Only the electricity procured through this contract will produce green hydrogen. In addition, the electrolyzer is connected to the grid and has the ability to buy electricity from the day-ahead market and to buy and sell from the intraday continuous market, and can provide secondary reserve (aFRR). Any MWh obtained from the grid will produce gray hydrogen. The considered use-case is presented in Figure 5. The left side of the picture represents the electricity bought (from the markets or the PPA) to power the electrolyzer. This electricity is consumed in the electrolysis process to produce hydrogen (right side of the figure). In addition, the electrolyzer can adjust its consumption profile to respond to the grid signal when providing secondary reserve. This is represented at the top of the figure. Any additional electricity consumed in this context participates toward gray H2 production. Regarding the value of hydrogen, a different price is set depending on whether the hydrogen can be qualified as "green" or not. The selling price of gray hydrogen is set at 2 €/kg, while the price for green

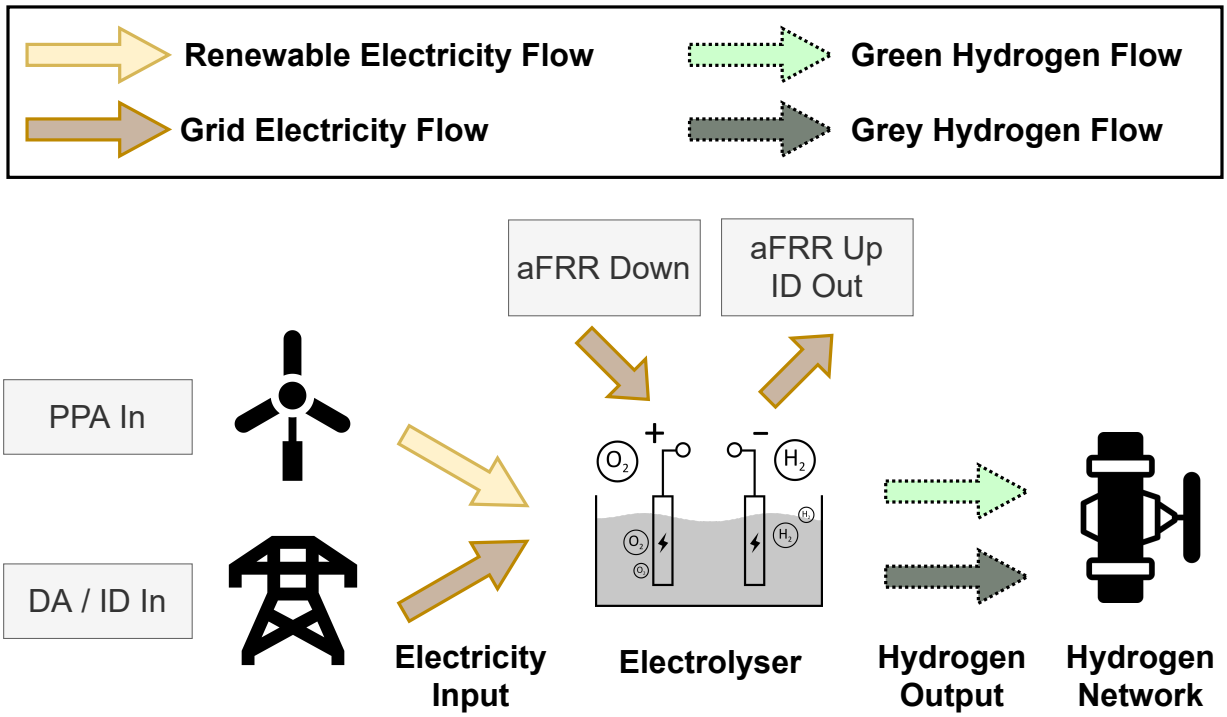

Figure 5: Electrolyzer use-case representation

hydrogen is set at 6 €/kg. Both prices are identified in ref Ji and Wang (2021) (The price for gray H2 is set at the same price as gray H2 produced using SMR units).

5.1. Component and market participation dimensioning

Regarding the size of the components, the electrolyzer has a rated power of 200 MW. Its minimal consumption is 10 MW, with the assumption that this operating power maintains the minimum current requirement Chardonnet (2017). The efficiency of the electrolyzer is set at 57 kWh/kg Proost (2019). The PPA contract is "as produced", meaning that a certain percentage of the rated power of the wind farm will be allocated to the electrolyzer. The size of the PPA contract is set at 200 MW. The plant has to manage its profile to follow this power input, or pay the corresponding imbalance fee if it cannot. The PPA contract price is set as an indexation of the spot price (discount to market with collar WBCSD (2021)). Each MWh of PPA is bought at 80% of the current spot price. To protect both producer and consumer, it is assumed that the PPA price is bounded within [40, 100] €/MWh against extreme electricity prices.

The secondary reserve allowed is set at 20MW combining contracted and non-contracted bids.

For the DA and Intraday markets, it is assumed that the plant will always manage to buy energy as long as the gate closure constraints are respected. For the day-ahead market, the clearing price will be the buying price. The plant cannot sell energy on the DA market.

A mixed pay-as-bid approach is assumed for the intraday market. The least favorable option between the bid price on the intraday market and the index price is taken when considering energy transactions. This is closest to reality since if the wanted price was not in line with the market but the plant still had to take a position on it, the market price would have to be accepted anyway. In this work, the German electricity markets and reserve mechanisms are considered, therefore the grid fees have been taken from one of the four German TSOs, 50Hertz. This grid fee amounts to 5€/MWh bought or sold on any electricity market noa (2020). This fee is included in the electricity price for every

transaction performed on the two electricity markets. The price relative to installed capacity is not considered in this work, as the investment costs of the assets are not considered.

Intraday participation is also constrained in both time and power. By allowing intraday participation too far in the future, the optimization problem can consider it a better option than day-ahead participation. It is however not the goal here to use intra-day market participation in a day-ahead fashion. Rather, the goal is to reposition the plant by following the evolution of the forecast errors. To do so, intraday participation is only allowed from 1 to 6 hours ahead of the current time-step. This prevents the optimization problem from replacing a day-ahead participation with an intraday bid perceived as better at the time of the day-ahead gate closure. The theoretical gate closure time for the intraday continuous market is T - 5 min to delivery. In this paper, we assume that the plant will not participate in the intraday market less than 1 h before delivery. The closer to gate closure, the lower the liquidity of the intraday market. This last constraint makes it easier to assume that the plant will always be able to buy power on the intraday market. Following the same reasoning, the maximal bid volume is set at 20 MW when participating in the ID market.

5.2. Data

Historical data for the year 2021 is used for the simulation. The wind power generation profile is built using open source data from Belgian offshore wind power plants, provided by Elia Elia. It is assumed that a fraction of the Belgian offshore production is bought using a PPA contract. The global offshore wind power output is normalized and scaled to have a power generation profile. The Belgian offshore wind production was chosen because it is the closest open data set to Germany. The goal is to capture as much correlation between wind generation and market quantities as possible. In addition, the Belgian offshore is all aggregated in a small geographical area, which makes it possible to forecast with weather data.

The secondary reserve bids and prices and the second-based aFRR data are extracted from the German TSO's reserve platform, Regelleistung.net Regelleistung for the year 2021. The spot and imbalance prices (Rebap) are obtained from the ENTSO-E transparency platform for the year 2021 ENTSO-E (a). Finally, the intraday prices for the year 2021 are obtained from the EPEX spot platform EPEX.

5.3. Forecast methods

Electricity market forecasting: This work considers many uncertain sources of information. On the first hand, market quantities are forecasted. This includes spot market prices, continuous intraday index prices, aFRR capacity prices, and energy activation ratios. On the second hand, the wind power provided by the wind farm is forecasted using meteorological data. The market quantities are forecasted using persistence approaches coupled with knowledge relative to the seasonal behavior of each market. Spot market prices are forecasted using prices from the last known day for each hour (the price at hour 08:00 for day D will be the price at hour 08:00 for day D-1). The intraday price will be constant over all time periods and will be equal to the last known intraday index price.

aFRR capacity reserve price forecast: Due to the pay-as-bid nature of this auction, a compromise has to be made between the absolute error regarding the price and the fact that if the forecasted price is higher than the marginal price for a given period, the plant will not be scheduled and the revenue will be zero. Therefore, purposefully aiming below the marginal price would increase the error and decrease the revenue while increasing the probability of being scheduled at the auction. To assess this, two persistence methods are compared to forecast the aFRR capacity price. The prices of the previous period are used (i.e. POS_00_04 for D-1 is used to forecast POS_00_04 for D). These two methods use the previous marginal price or the previous average price for a given period. They are respectively called "Marginal" and "Average". Since the average price is lower than the marginal price, using it to forecast the next day's marginal price increases the probability of being scheduled, but reduces the revenue when scheduled.

Wind power production forecast: A probabilistic forecast of wind power production was derived using a state-of-the-art quantile regression approach known to be effective for wind forecasting, namely Quantile Regression Forests (QRF) Camal (2020). The model predicts the production of the target wind site depending on two types of explanatory variables known to be relevant for hours-ahead to day-ahead horizons, recent lags of observed production, and Numerical Weather Predictions Petropoulos et al. (2022). The QRF is trained for each horizon in the horizon range H={15 min, 30 min, ..., 48 h} and predicts the following quantiles of the expected distribution: {5%, 10%, ..., 50%,

Table 1: Spot and intraday price forecast comparison for the year 2021

	Bias	MAE	RMSE
Spot Market	0.1	25.33	43.79
Intraday Market	0	14.86	24.24

Table 2: Positive aFRR capacity price forecast comparison for the years 2020 and 2021

	Sched. (%)	Av. Rev. (€/MW)	Bias	MAE	RMSE
Perfect	100.0	21.66	0	0	0
Marginal	34.2	3.28	0	18.89	107.13
Average	72.8	6.47	-11.36	12.62	81.51

..., 95%}. The regression model parameters i.e. number of trees, and the number of variables considered per split are tuned by cross-validation in a training-validation set spanning over the year 2020, then predictions are issued for the year 2021.

The model predicts the total production of the multiple offshore wind farms in Belgium, concentrated in a geographical area small enough to be approximated as a single large production site. The predicted wind speeds and the air temperature across the NWP grid points covering the different offshore farms are retrieved from ECMWF HRES at 00h00 runtimes and hourly lead-times up to the maximum horizon in the horizon range H. The target variable of the regression is the total active production. It is scaled by the total installed capacity, which is reported to increase monotonously in the training and testing set but is not affected to the different farms in the offshore portfolio. The uncertainty on this affectation creates significant bias in the model, but further forecasting improvements are out of the scope of this paper and the results reported below are sufficient for the considered application.

5.4. Forecast analysis

Electricity markets forecast: The quality of the electricity market price forecasting is assessed using the bias, MAE and RMSE metrics. The results are presented in Table 1. For both markets, the bias is very close to zero, most likely due to the persistence nature of the forecasting method. In addition, the forecasting is better for the intraday market. This can be explained by the fact that the prices for the intraday market are all forecasted one hour ahead, when the decision regarding the placement of the bids is final. The bids on the spot market on the other hand have to be placed at 12:00 D-1 for the whole day D, therefore the lead time goes from 12 to 36 hours ahead.

aFRR forecast: The comparisons of the results for the two aFRR capacity prices forecasts are presented in Table 2 and Table 3 for positive and negative aFRR prices respectively. Forecasting these prices using the previous average price consistently performs better than using the previous marginal price. For both directions, the bias indicates that we are under-evaluating the price using the previous average price, but this increases the amount of time the bid is actually accepted, therefore increasing the average capacity revenue.

Table 3: Negative aFRR capacity price forecast comparison for the years 2020 and 2021

	Sched. (%)	Av. Rev. (€/MW)	Bias	MAE	RMSE
Perfect	100.0	23.04	0	0	0
Marginal	43.4	3.41	-0.01	24.01	290.42
Average	78.7	5.57	-13.97	16.10	210.07

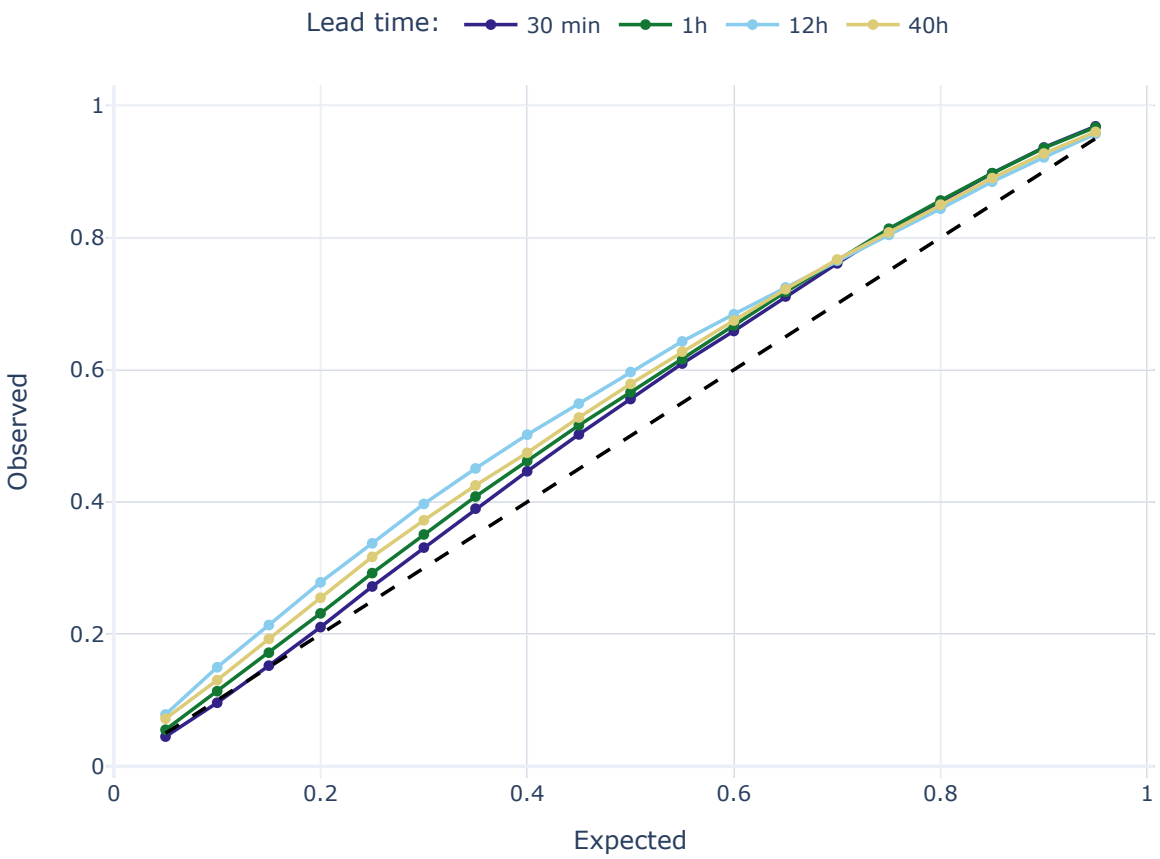

Figure 6: Probabilistic wind forecast reliability diagram

Wind probabilistic forecast: In this section we analyze the quality of the wind forecast using QRF with NWP. A reliability diagram can be found in Figure 6 and sharpness and NRMSE diagrams in Figure 7. It can be observed that the forecast tends to under-evaluate the quantiles (more values are observed below a given quantile than would be expected). This under-evaluation increases as the quantiles become less extreme. This bias also generally increases with the lead time. The quantile interval size and NRMSE quickly rise up to a 4 h lead time, and then continue to increase less sharply. This leads to a better performance of the forecast for shorter lead times, hence increasing the quality of repositioning on the intraday market.

5.5. Market price distribution and month selection

A set of months representing the possible state of market prices is selected for the analysis. The goal is to represent both extremes in terms of electricity and reserve prices. To do so, the monthly distributions of the spot and intraday market prices are represented in Figure 8. We can observe the impact of the energy crisis that started at the end of 2021, reflected in the increase in the average price and the variance of the prices as the year goes by. A similar distribution analysis is performed on the capacity prices for the aFRR in both directions, shown in Figure 9. For the reserve prices, no particular trend can be observed in the distributions. However, the capacity reserve prices can vary greatly from one month to the next.

For the analysis, four months have been selected: January, February, October, and December. The first two are months presenting low electricity market prices, while January presents low reserve prices and February high reserve prices. The last two months show high electricity market prices, with October presenting high reserve prices and December low reserve prices.

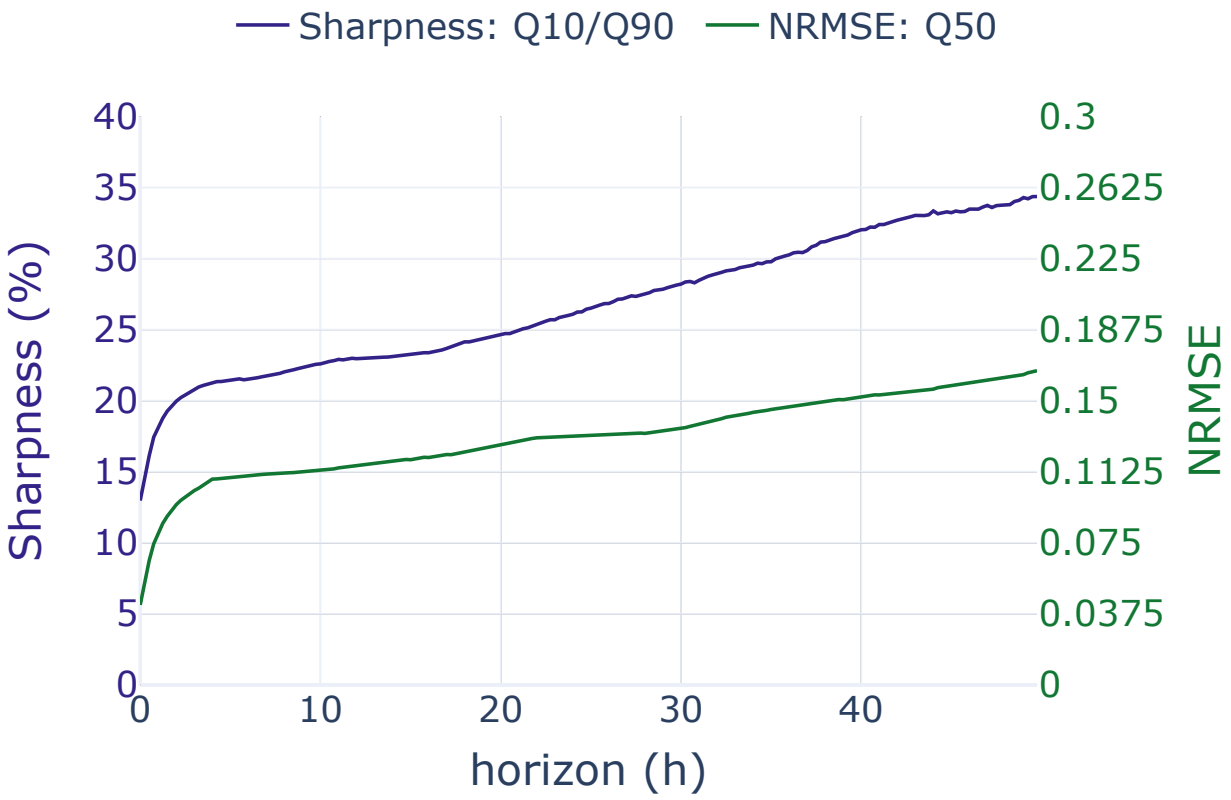

Figure 7: Probabilistic wind forecast sharpness and Q50 NRMSE

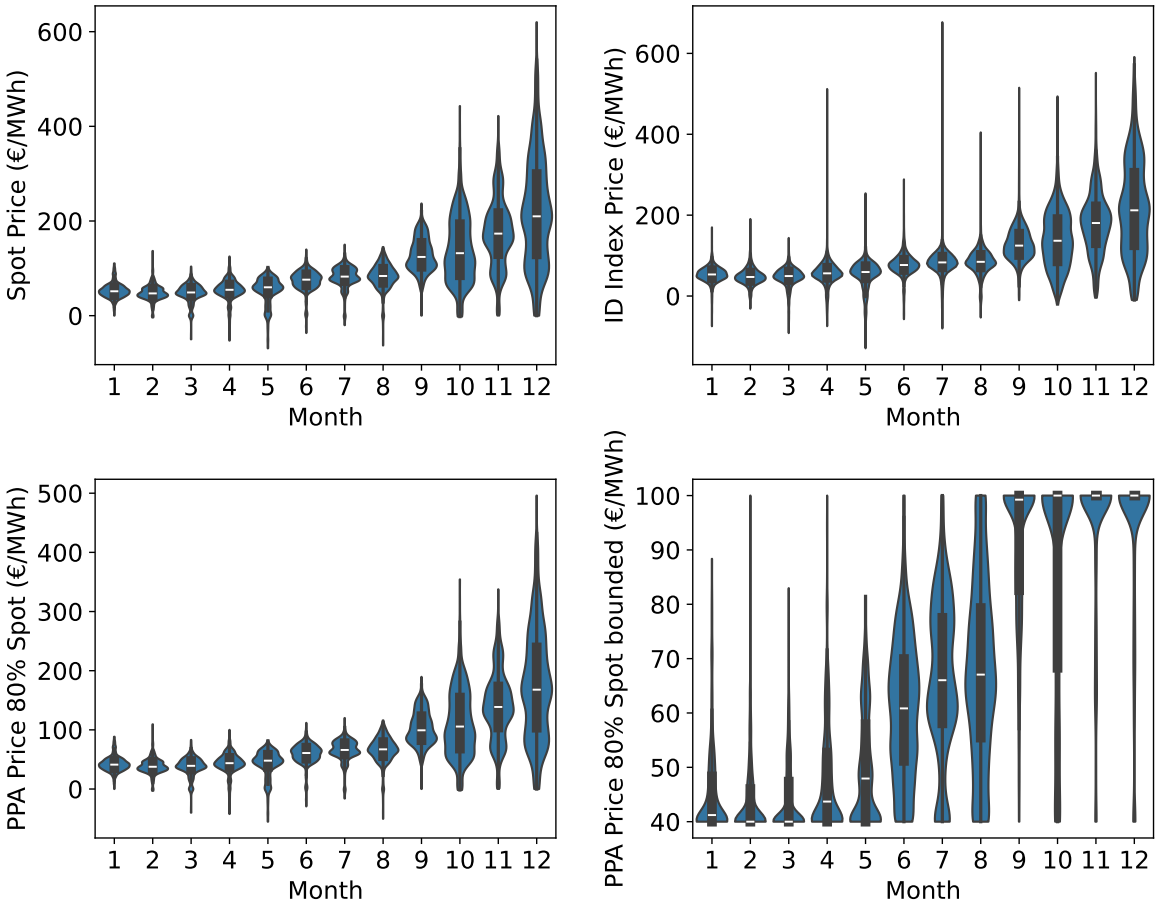

Figure 8: Monthly price distribution for each market and PPA contracts for the year 2021

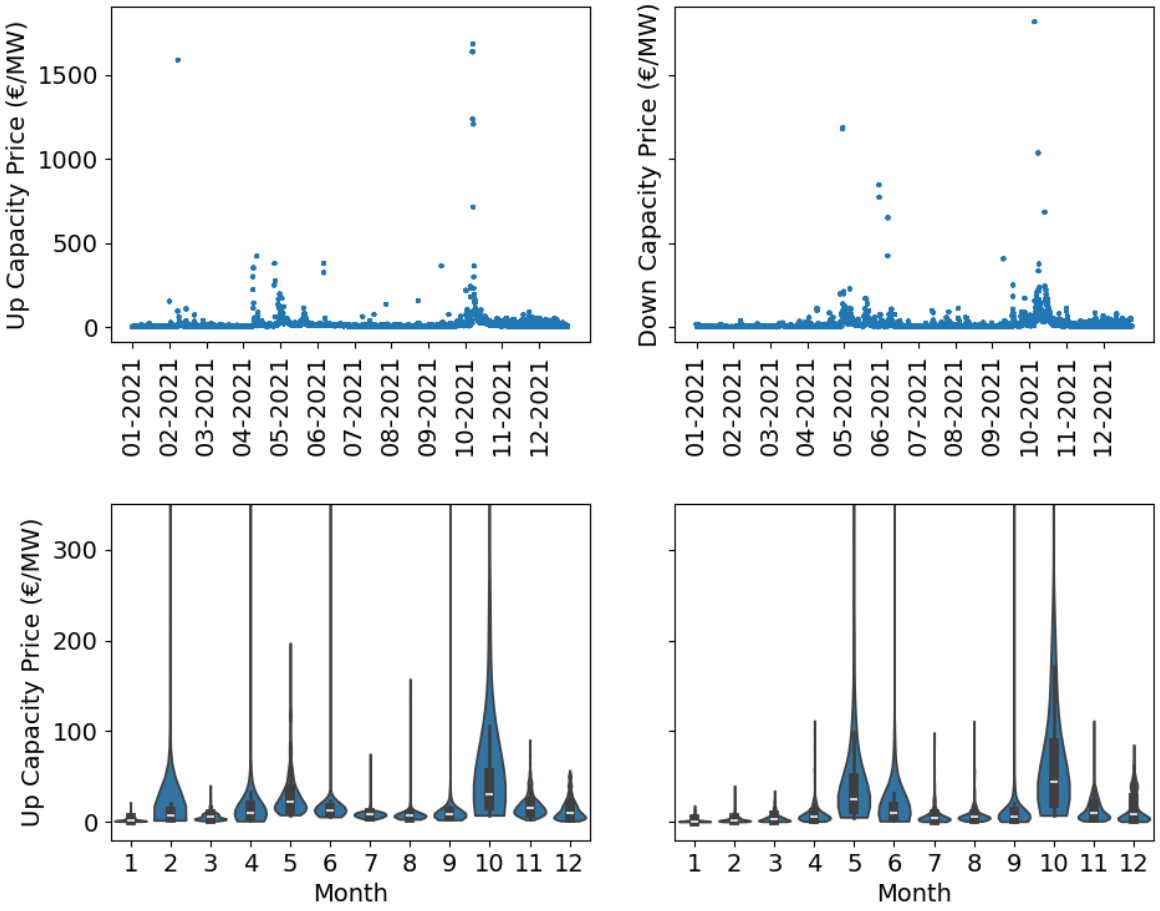

Figure 9: Monthly reserve price distribution for each reserve direction for the year 2021. In the lower part of the figure, extreme prices are cropped to better display the distribution. These prices are shown in the upper scatter plots

Table 4: Statistics on the cash flow per period for the base case for the year 2021

Cash Flow (€/15min)	Perfect	Det.	Robust
Mean	735	682	670
std	872	900	884
95%-Var	-1365	-1402	-1407
95%-CVar	-1437	-1790	-1684

Table 5: Statistics on the cash flow per period for the full case for the year 2021

Cash Flow (€/15min)	Perfect	Det.	Robust
Mean	1600	900	845
std	2061	1168	1159
95%-Var	-1184	-1459	-1496
95%-CVar	-1331	-1801	-1813

6. Results

For each month of 2021, we run the algorithm for two cases. The base case will serve as a reference. It will only consider the electrolyzer powered through the PPA, with a day-ahead market participation to handle the volatility of the renewable power source. The full case will consider that the participation comprises all the market and services (PPA, day-ahead, intraday, and secondary reserve). For each case, three uncertainty management strategies are considered. First, the perfect knowledge approach will consider no uncertainty, therefore putting an upper limit on the potential of each market participation strategy. The deterministic and robust runs will then be compared to assess the pros and cons of each approach.

6.1. Cash flow analysis

The cash flow for each monthly run is extracted and averaged per 15-min period over the whole year. The corresponding results are shown for the base case and the full case in Table 4 and Table 5 respectively. When comparing the average cash flow for a given strategy in the full case with the corresponding strategy in the base case, the addition of the reserve and intraday participation presents better results. The standard deviation of the average cash flow also increases accordingly. This can be explained by the higher volatility in revenues due to the changing reserve prices. In addition, a higher increase in standard deviation is observed in the perfect knowledge strategy compared to the uncertain strategies, due to the better utilization of the extreme reserve prices. Regarding exposure to risk, the Var and CVar are higher when adding the reserve and ID participation for the uncertain cases, but lower when considering the perfect knowledge approach. This shows that reserve provision reduces the risk exposure with a perfect knowledge assumption, but increases it when accounting for the uncertainty. Overall, the robust approach appears to show slightly worse results when compared to the deterministic approach. This is to be expected, as the robust approach is more conservative, and focuses on avoiding imbalances, at the cost of lost opportunities.

Figure 10 shows the monthly averaged cash flow for each strategy in both the full case and the base case. We can observe that the difference between strategies is limited when considering the base case. When considering the full case, the uncertain approaches show similar performances and follow a similar trend to the one observed in the base case. The perfect knowledge strategy makes the most of the revenue potential of the reserve, therefore drastically increasing the cash flow. This is especially true in October, which shows extreme reserve prices, as previously seen in Figure 9.

To assess the performance of the full case against the base case, Figure 11 shows the cash flow increase per month, for each of the strategies, as a percentage of the base case cash flow. The perfect knowledge strategies once again

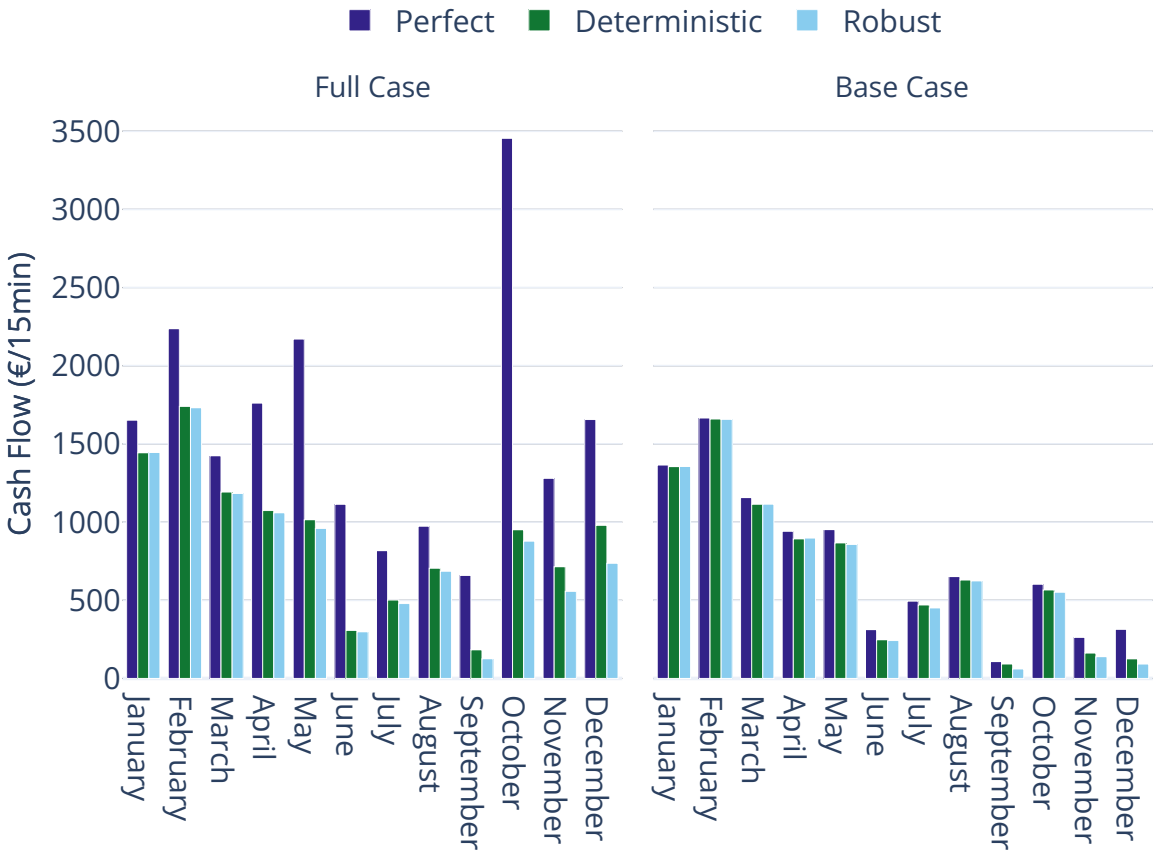

Figure 10: Cash flow comparison between uncertainty management approaches for both the full and the base cases

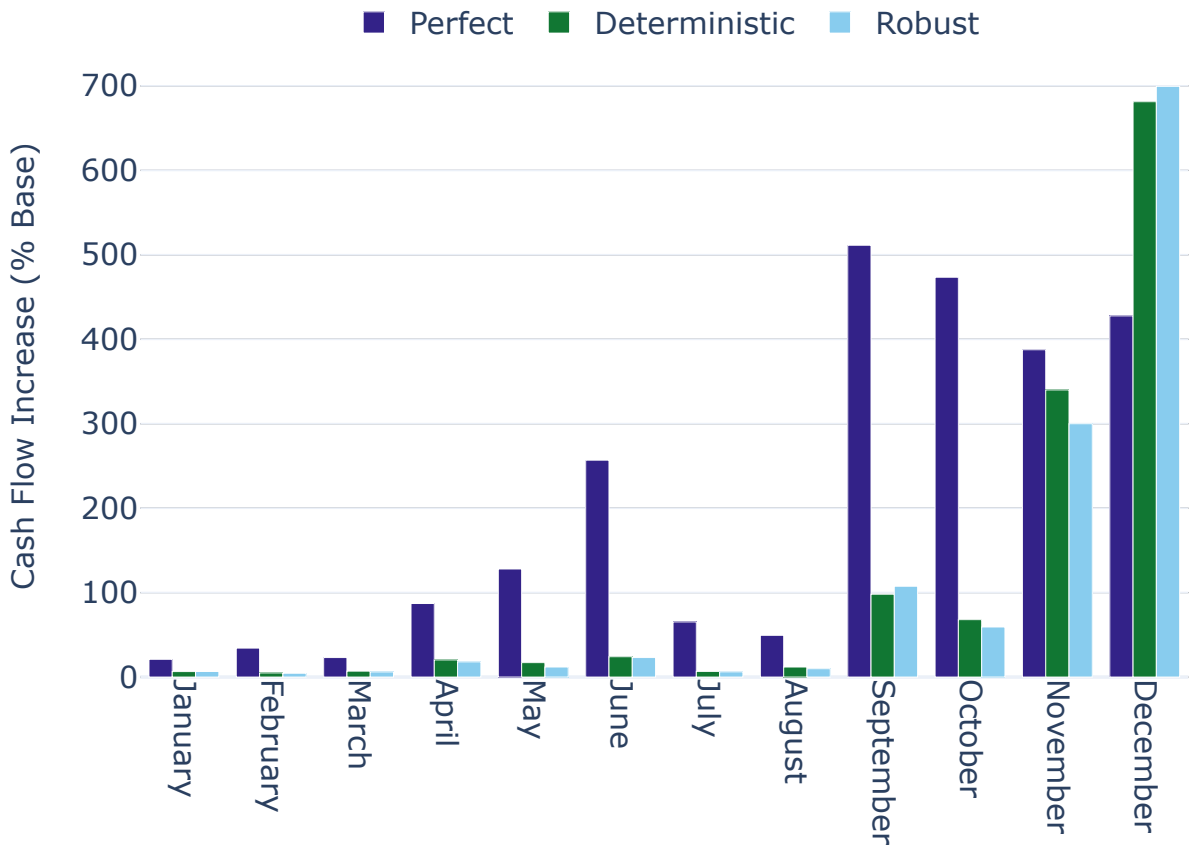

Figure 11: Cash flow increase between uncertainty management approaches of the full case as a percentage of the base case

drastically outperform both uncertain strategies, except for the last two months of the year. This shows that the addition of the reserve provision is a good tool to compensate lower revenues due to large electricity prices. To illustrate this, the same data has been averaged over two periods of the year. First, before the crisis until August, when the spot and intraday prices were still within the expected market price range. Second, after August, when the market prices started skyrocketing, and finally over the whole year. These results are shown in Table 6. This table shows an increase in performance of around 10% before the crisis for both uncertain strategies, whereas the same strategies show an increase of more than 290% on average during the crisis. The perfect knowledge approach also shows a large increase during the crisis, but this is to be expected, as the algorithm can take advantage of extreme market prices (both high and low).

6.2. Imbalance analysis

The revenue analysis shows slightly worse performances when considering the robust approach compared to the deterministic approach. However, the revenue analysis does not account for the behavior of the algorithm in terms of imbalances. Indeed, due to the one-price settlement of the balancing mechanism, the plant can generate profit when out of balance. This however is not a situation in which an actor wants to be, as it is very hard to forecast which way the prices will go, therefore exposing the plant to large imbalance costs. In addition, plants subject to frequent imbalances can receive additional penalties. The robust approach focuses on reducing the risk of imbalance when running the optimization, at the cost of higher conservatism and lost opportunities. Table 7 and Table 8 show statistics on the imbalance averaged per period for each strategy for the base case and the full case respectively. As expected, the perfect knowledge approach shows no imbalance. Regarding the uncertain strategies, the robust approach drastically

Table 6: Average percentage of increase per month between full case and base case, before the crisis, during the crisis, and over the whole year, using the data shown in Figure 11

Cash Flow Increase (%)	Perfect	Det.	Robust
Until August	83	12	10
After August	450	297	292
Whole Year	205	107	104

Table 7: Statistics on the imbalance count and average volumes per period for the base case for the year 2021

Imbalance (MW)	Perfect	Det.	Robust
Occurence (%)	0.0	2.24	0.78
Av. Imb. Vol.	0.0	9.33	4.47
95%-Var	0.0	15.43	10.75
95%-CVar	0.0	26.02	18.08

reduces the percentage of occurrence of periods when the plant finds itself in imbalance, as well as the average volume of imbalance. The risk exposure is also reduced when looking at the volume of imbalance.

6.3. Green Hydrogen Strike Price Analysis

Finally, we compare the breakeven price for green H2 for each case and strategy with the formula shown in Equation (33).

$$V^{strike} = V^{green} - \frac{R^{Tot}}{\sum_t^T Q_t^{H2,green}} \tag{33}$$

Figure 12 shows the monthly average value of the H2 breakeven price for both the full case and the base case, for each of the three strategies. For the best case, all three strategies behave similarly, as they are mostly driven by market prices. This induces an increase in the breakeven price as the year goes by and the crisis appears. The perfect knowledge strategy and both uncertain strategies show this price to be above the originally fixed price of 6 €/kg for 5 and 6 months of the year 2021 respectively (most of them after August). For the full case, the uncertain strategies show 5 months with a breakeven price above 6 €/kg. The perfect strategy drastically outperforms the other two, with most of the breakeven prices being negative (meaning that the revenue obtained through the reserve provision is greater than the cost of the electricity used to produce H2).

Table 8: Statistics on the imbalance count and average volumes per period for the full case for the year 2021

Imbalance (MW)	Perfect	Det.	Robust
Occurence (%)	0.0	1.49	0.28
Av. Imb. Vol.	0.0	6.01	3.40
95%-Var	0.0	18.22	12.00
95%-CVar	0.0	26.58	16.78

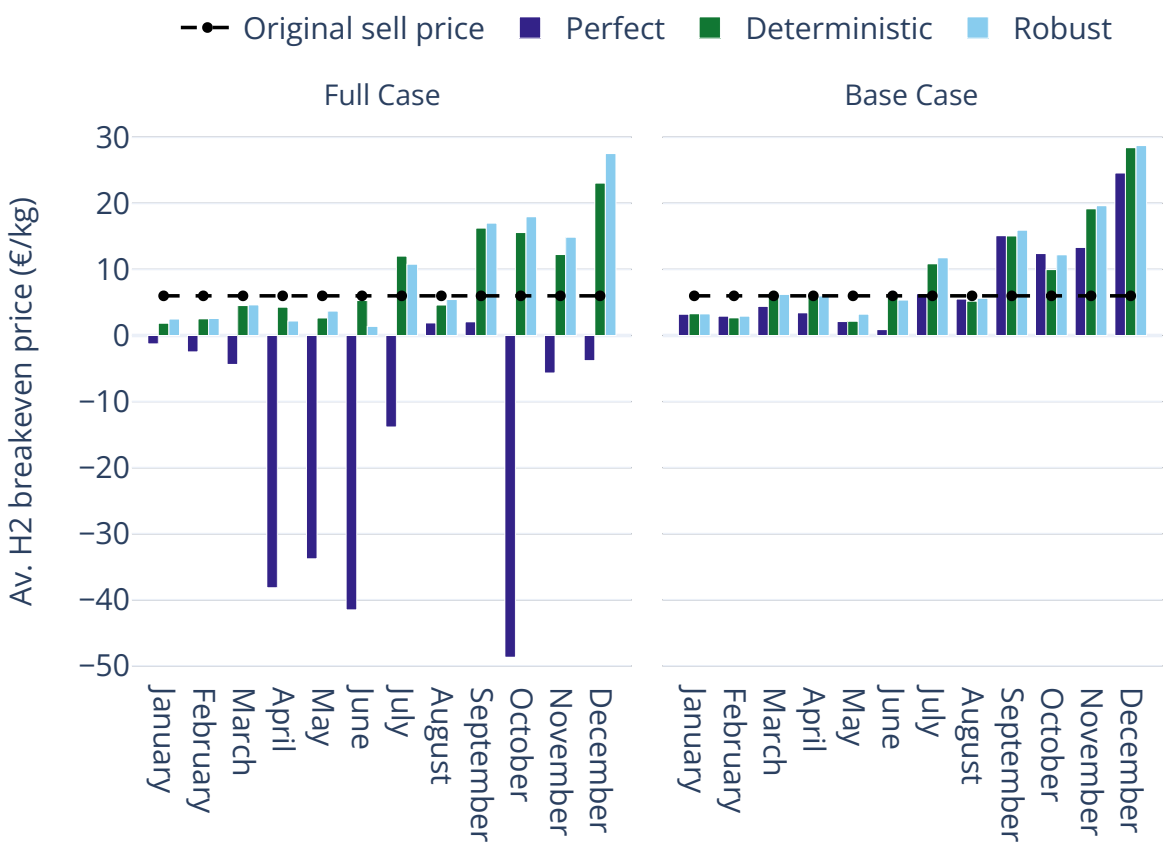

Figure 12: H2 breakeven price comparison between uncertainty management approaches for both the full case and the base case

Table 9: Absolute decrease in the green H2 breakeven price for the full case compared to the base case (to account for negative breakeven prices)

Breakeven price Decrease (%)	Perfect	Det.	Robust
Until August	563.91	10.08	25.21
After August	185.77	7.55	-1.11
Whole Year	301.34	8.47	8.55

The percentage of absolute decrease (to account for negative value) in breakeven prices between the full case and the base case before and during the crisis as well as for the whole year is shown in Table 9. As expected, it shows a very large improvement for all three periods. Both uncertain strategies show an improvement before the crisis, with the robust approach showing better performances. However, the robust approach also shows a negative performance compared to the base case in time of crisis, which means that the robust approach actually increases the breakeven price of the green H2 in this period and therefore has a negative impact.

7. Conclusions

This paper proposed an economic analysis of an electrolyzer providing grid services combined with multi-market participation. Optimization under uncertainty was combined with a rolling horizon algorithm to simulate the day-to-day operation of the plant. Multiple uncertain sources were considered and market rules were implemented to model the expected trading behavior as close as possible to real life. Deterministic and robust formulations were used to account for uncertainties in renewable generation and market prices, and the results of both approaches were compared. This algorithm was run over the year 2021 for two market participation strategies both in perfect knowledge and uncertain contexts. The cash flow, the imbalance volumes and frequency, and the green H2 breakeven price are the three performance indicators considered for the performance analysis of each scenario. The revenue analysis shows that the addition of secondary reserve provision increases the mean cash flow of both uncertain approaches, with a slight advantage going to the deterministic approach. However, it is also observed that adding the reserve provision increases the risk exposure when accounting for uncertainties. Regarding the performances in times of crisis (at the end of 2021), the addition of reserve provisions greatly increases the performances of the uncertain strategies ($\sim$ 300 % cash flow increase for the full case compared to the base case, against $\sim$ 10% before the crisis). The imbalance analysis shows much better performances from the robust approach in terms of percentage of occurrence, average imbalance volumes, and risk exposure. In terms of the effect on the breakeven price of green H2, both uncertain approaches show similar yearly performances of around an 8.5% decrease in price compared to the base case. However, the robust approach performs much better before the start of the crisis (25% reduction against 10% for the deterministic approach), whereas it shows a negative performance compared to the base case with a 1.1% increase in the breakeven price, and the deterministic approach still shows an improvement with a 7.55 % decrease in the breakeven price. Finally, the perfect knowledge strategy shows a very high potential in all the performance indicators, with much better performances than its uncertain counterparts. This approach even shows a negative green H2 breakeven price, meaning that the perfect knowledge participation in the reserve alone more than compensates the cost of buying renewable power to produce hydrogen. This shows the potential benefits that would come from higher forecast quality, especially in the secondary reserve quantities.

References

, . Air Liquide Normand'Hy Project. URL: https://normandhy.airliquide.com/en/air-liquide-normandhy/project-heart-normandy-industrial-basin.

, 2020. 50Hertz Grid Access Price Sheet 2021. URL: https://www.50hertz.com/en/Partners/Gridcustomers/Gridaccess.

Al-Lawati, R.A., Crespo-Vazquez, J.L., Faiz, T.I., Fang, X., Noor-E-Alam, M., 2021. Two-stage stochastic optimization frameworks to aid in decision-making under uncertainty for variable resource generators participating in a sequential energy market. Applied Energy 292, 116882. doi:10.1016/j.apenergy.2021.116882.

Baetens, J., De Kooning, J.D.M., Van Eetvelde, G., Vandevelde, L., 2020. A Two-Stage Stochastic Optimisation Methodology for the Operation of a Chlor-Alkali Electrolyser under Variable DAM and FCR Market Prices. Energies 13, 5675. doi:10.3390/en13215675. number: 21 Publisher: Multidisciplinary Digital Publishing Institute.

Baumhof, M.T., Raheli, E., Johnsen, A.G., Kazempour, J., 2023. Optimization of Hybrid Power Plants: When Is a Detailed Electrolyzer Model Necessary? ArXiv:2301.05310 [cs, eess, math].

Bergen, A., Pitt, L., Rowe, A., Wild, P., Djilali, N., 2009. Transient electrolyser response in a renewable-regenerative energy system. International Journal of Hydrogen Energy 34, 64–70. doi:10.1016/j.ijhydene.2008.10.007.

Camal, S., 2020. Forecasting and optimization of ancillary services provision by renewable energy sources. phdthesis. Université Paris sciences et lettres. URL: https://pastel.archives-ouvertes.fr/tel-02973808.

Chardonnet, C., 2017. Study on Early Business Cases for H2 in Energy Storage and More Broadly Power to H2 Applications. URL: https://hsweb.hs.uni-hamburg.de/projects/star-formation/hydrogen/P2H_Full_Study_FCHJU.pdf.

Commission, E., 2022. Joint European action for more affordable, secure energy. URL: https://ec.europa.eu/commission/presscorner/detail/en/ip_22_1511.

Dadkhah, A., Bozalakov, D., De Kooning, J.D., Vandevelde, L., 2021. On the optimal planning of a hydrogen refuelling station participating in the electricity and balancing markets. International Journal of Hydrogen Energy 46, 1488–1500. doi:10.1016/j.ijhydene.2020.10.130.

Dadkhah, A., Bozalakov, D., De Kooning, J.D.M., Vandevelde, L., 2022. Techno-Economic Analysis and Optimal Operation of a Hydrogen Refueling Station Providing Frequency Ancillary Services. IEEE Transactions on Industry Applications 58, 5171–5183. doi:10.1109/TIA.2022.3167377.

Ding, H., Hu, Z., Song, Y., 2015. Rolling Optimization of Wind Farm and Energy Storage System in Electricity Markets. IEEE Transactions on Power Systems 30, 2676–2684. doi:10.1109/TPWRS.2014.2364272.

Dozein, M.G., Jalali, A., Mancarella, P., 2021. Fast Frequency Response From Utility-Scale Hydrogen Electrolyzers. IEEE Transactions on Sustainable Energy 12, 1707–1717. doi:10.1109/TSTE.2021.3063245.

Dudurych, I.M., 2021. The Impact of Renewables on Operational Security: Operating Power Systems That Have Extremely High Penetrations of Nonsynchronous Renewable Sources. IEEE Power and Energy Magazine 19, 37–45. doi:10.1109/MPE.2020.3043614.

Elia, . Elia Open Data Portal. URL: https://opendata.elia.be/pages/home/.

ENTSO-E, a. ENTSO-E Transparency Platform. URL: https://transparency.entsoe.eu/.

ENTSO-E, b. PICASSO Project. URL: https://www.entsoe.eu/network_codes/eb/picasso/.

ENTSO-E, 2021. MARI PICASSO Stakeholder Workshop. URL: https://www.entsoe.eu/events/2021/12/02/picasso-mari-stakeholder-workshop/.

EPEX, . EPEX SPOT. URL: https://www.epexspot.com/en.

Gorissen, B.L., Yanıkoğlu, I., Hertog, D.d., 2015. A Practical Guide to Robust Optimization. Omega 53, 124–137. doi:10.1016/j.omega.2014.12.006. arXiv:1501.02634 [math].

Gu, C., Tang, C., Xiang, Y., Xie, D., 2019. Power-to-gas management using robust optimisation in integrated energy systems. Applied Energy 236, 681–689. doi:10.1016/j.apenergy.2018.12.028.

IEA, 2019. The Future of Hydrogen – Analysis. URL: https://www.iea.org/reports/the-future-of-hydrogen.

IEA, 2021a. Global Hydrogen Review 2021 – Analysis. URL: https://www.iea.org/reports/global-hydrogen-review-2021.

IEA, 2021b. Net Zero by 2050 – Analysis. URL: https://www.iea.org/reports/net-zero-by-2050.

IRENA, 2020. Green Hydrogen Cost Reduction: Scaling up Electrolysers to Meet the 1.5 degree C Climate Goal. URL: https://www.irena.org/publications/2020/Dec/Green-hydrogen-cost-reduction.

Ji, M., Wang, J., 2021. Review and comparison of various hydrogen production methods based on costs and life cycle impact assessment indicators. International Journal of Hydrogen Energy 46, 38612–38635. doi:10.1016/j.ijhydene.2021.09.142.

Martínez-Rodríguez, A., Abánades, A., 2020. Comparative Analysis of Energy and Exergy Performance of Hydrogen Production Methods. Entropy 22, 1286. doi:10.3390/e22111286.

Massana, J., Burgas, L., Herraiz, S., Colomer, J., Pous, C., 2022. Multi-vector energy management system including scheduling electrolyser, electric vehicle charging station and other assets in a real scenario. Journal of Cleaner Production 380, 134996. doi:10.1016/j.jclepro.2022.134996.

Petropoulos, F., Apiletti, D., Assimakopoulos, V., Babai, M.Z., Barrow, D.K., Ben Taieb, S., Bergmeir, C., Bessa, R.J., Bijak, J., Boylan, J.E., Browell, J., Carnevale, C., Castle, J.L., Cirillo, P., Clements, M.P., Cordeiro, C., Cyrino Oliveira, F.L., De Baets, S., Dokumentov, A., Ellison, J., Fiszeder, P., Franses, P.H., Frazier, D.T., Gilliland, M., Gönül, M.S., Goodwin, P., Grossi, L., Grushka-Cockayne, Y., Guidolin, M., Guidolin, M., Gunter, U., Guo, X., Guseo, R., Harvey, N., Hendry, D.F., Hollyman, R., Januschowski, T., Jeon, J., Jose, V.R.R., Kang, Y., Koehler, A.B., Kolassa, S., Kourentzes, N., Leva, S., Li, F., Litsiou, K., Makridakis, S., Martin, G.M., Martinez, A.B., Meeran, S., Modis, T., Nikolopoulos, K., Önkal, D., Paccagnini, A., Panagiotelis, A., Panapakidis, I., Pavía, J.M., Pedio, M., Pedregal, D.J., Pinson, P., Ramos, P., Rapach, D.E., Reade, J.J., Rostami-Tabar, B., Rubaszek, M., Sermpinis, G., Shang, H.L., Spiliotis, E., Syntetos, A.A., Talagala, P.D., Talagala, T.S., Tashman, L., Thomakos, D., Thorarinsdottir, T., Todini, E., Trapero Arenas, J.R., Wang, X., Winkler, R.L., Yusupova, A., Ziel, F., 2022. Forecasting: theory and practice. International Journal of Forecasting 38, 705–871. doi:10.1016/j.ijforecast.2021.11.001.

Proost, J., 2019. State-of-the art CAPEX data for water electrolysers, and their impact on renewable hydrogen price settings. International Journal of Hydrogen Energy 44, 4406–4413. doi:10.1016/j.ijhydene.2018.07.164.

Regelleistung, . Regelleistung Open Data Portal. URL: https://www.regelleistung.net/apps/datacenter/tenders/.

Sahin, F., Narayanan, A., Robinson, E.P., 2013. Rolling horizon planning in supply chains: review, implications and directions for future research. International Journal of Production Research 51, 5413–5436. doi:10.1080/00207543.2013.775523.

Samani, A.E., D'Amicis, A., De Kooning, J.D., Bozalakov, D., Silva, P., Vandevelde, L., 2020. Grid balancing with a large-scale electrolyser providing primary reserve. IET Renewable Power Generation 14, 3070–3078. doi:10.1049/iet-rpg.2020.0453.

Scolaro, M., Kittner, N., 2022. Optimizing hybrid offshore wind farms for cost-competitive hydrogen production in Germany. International Journal of Hydrogen Energy 47, 6478–6493. doi:10.1016/j.ijhydene.2021.12.062.

Seck, G.S., Hache, E., Sabathier, J., Guedes, F., Reigstad, G.A., Straus, J., Wolfgang, O., Ouassou, J.A., Askeland, M., Hjorth, I., Skjelbred, H.I.,

Andersson, L.E., Douguet, S., Villavicencio, M., Trüby, J., Brauer, J., Cabot, C., 2022. Hydrogen and the decarbonization of the energy system in europe in 2050: A detailed model-based analysis. Renewable and Sustainable Energy Reviews 167, 112779. doi:10.1016/j.rser.2022.112779.

Wang, J., Zhong, H., Tang, W., Rajagopal, R., Xia, Q., Kang, C., Wang, Y., 2017. Optimal bidding strategy for microgrids in joint energy and ancillary service markets considering flexible ramping products. Applied Energy 205, 294–303. doi:10.1016/j.apenergy.2017.07.047.

WBCSD, 2021. Pricing structures for corporate renewable PPAs. Technical Report. URL: https://www.wbcsd.org/Programs/Climate-and-Energy/Energy/REscale/Resources/Pricing-structures-for-corporate-renewable-PPAs.

Weiß, A., Siebel, A., Bernt, M., Shen, T.H., Tileli, V., Gasteiger, H.A., 2019. Impact of Intermittent Operation on Lifetime and Performance of a PEM Water Electrolyzer. Journal of The Electrochemical Society 166, F487–F497. doi:10.1149/2.0421908jes.

Wu, X., Zhao, W., Li, H., Liu, B., Zhang, Z., Wang, X., 2021. Multi-stage stochastic programming based offering strategy for hydrogen fueling station in joint energy, reserve markets. Renewable Energy 180, 605–615. doi:10.1016/j.renene.2021.08.076.

Ziarnetzky, T., Mönch, L., Uzsoy, R., 2018. Rolling horizon, multi-product production planning with chance constraints and forecast evolution for wafer fabs. International Journal of Production Research 56, 6112–6134. doi:10.1080/00207543.2018.1478461.